



ARL-TN-0774 • SEP 2016



Sensitivity Analysis and Simulation of Theoretical Response of Ceramics to Strong Magnetic Fields

**by Carli A Moorehead, Michael M Kornecki, Victoria L Blair,
Raymond E Brennan**

Approved for public release; distribution is unlimited.

NOTICES

Disclaimers

The findings in this report are not to be construed as an official Department of the Army position unless so designated by other authorized documents.

Citation of manufacturer's or trade names does not constitute an official endorsement or approval of the use thereof.

Destroy this report when it is no longer needed. Do not return it to the originator.



Sensitivity Analysis and Simulation of Theoretical Response of Ceramics to Strong Magnetic Fields

by Carli A Moorehead

Drexel University, Philadelphia, Pennsylvania

Michael M Kornecki, Victoria L Blair, and Raymond E Brennan

Weapons and Materials Research Directorate, ARL

REPORT DOCUMENTATION PAGE				Form Approved OMB No. 0704-0188	
<p>Public reporting burden for this collection of information is estimated to average 1 hour per response, including the time for reviewing instructions, searching existing data sources, gathering and maintaining the data needed, and completing and reviewing the collection information. Send comments regarding this burden estimate or any other aspect of this collection of information, including suggestions for reducing the burden, to Department of Defense, Washington Headquarters Services, Directorate for Information Operations and Reports (0704-0188), 1215 Jefferson Davis Highway, Suite 1204, Arlington, VA 22202-4302. Respondents should be aware that notwithstanding any other provision of law, no person shall be subject to any penalty for failing to comply with a collection of information if it does not display a currently valid OMB control number.</p> <p>PLEASE DO NOT RETURN YOUR FORM TO THE ABOVE ADDRESS.</p>					
1. REPORT DATE (DD-MM-YYYY) September 2016		2. REPORT TYPE Technical Note		3. DATES COVERED (From - To) 1 March–30 June 2016	
4. TITLE AND SUBTITLE Sensitivity Analysis and Simulation of Theoretical Response of Ceramics to Strong Magnetic Fields				5a. CONTRACT NUMBER	
				5b. GRANT NUMBER	
				5c. PROGRAM ELEMENT NUMBER	
6. AUTHOR(S) Carli A Moorehead, Michael M Kornecki, Victoria L Blair, and Raymond E Brennan				5d. PROJECT NUMBER DSI-14-WMR-014	
				5e. TASK NUMBER	
				5f. WORK UNIT NUMBER	
7. PERFORMING ORGANIZATION NAME(S) AND ADDRESS(ES) US Army Research Laboratory ATTN: RDRL-WMM-E Aberdeen Proving Ground, MD 21005-5069				8. PERFORMING ORGANIZATION REPORT NUMBER ARL-TN-0774	
9. SPONSORING/MONITORING AGENCY NAME(S) AND ADDRESS(ES)				10. SPONSOR/MONITOR'S ACRONYM(S)	
				11. SPONSOR/MONITOR'S REPORT NUMBER(S)	
12. DISTRIBUTION/AVAILABILITY STATEMENT Approved for public release; distribution is unlimited.					
13. SUPPLEMENTARY NOTES					
14. ABSTRACT <p>Equations governing the response of materials to an applied magnetic field can be derived from first principles. Using the derived equations, computer models (MATLAB) were designed to investigate and predict the response of specific materials and experimental conditions to applied magnetic fields. Using the generated computer models, the time required for alignment is predicted to be 35–55 s for epoxy and gel-casting suspensions at relatively low (1.8 T) applied magnetic fields. This corresponds well to preliminary experimental results. Additionally, the sensitivity of magnetic response to process variables, such as variations in applied magnetic field and suspension viscosity, is assessed. Results indicate that changes in the applied magnetic field strength are most effective for improving alignment and could be the source of experimental variation if the consistency of the applied field is not carefully controlled.</p>					
15. SUBJECT TERMS magnetic alignment, simulation, micro-texture, magnetic field processing, alumina					
16. SECURITY CLASSIFICATION OF:			17. LIMITATION OF ABSTRACT UU	18. NUMBER OF PAGES 24	19a. NAME OF RESPONSIBLE PERSON Carli A Moorehead
a. REPORT Unclassified	b. ABSTRACT Unclassified	c. THIS PAGE Unclassified			19b. TELEPHONE NUMBER (Include area code) 410-306-4397

Contents

List of Figures	iv
List of Tables	iv
1. Introduction	1
2. Methods	2
2.1 Defining Parameters	2
2.2 Magnetic Response Predictions	3
2.3 Sensitivity Analysis	3
3. Results and Discussion	4
3.1 Magnetic Response Predictions	4
3.2 Sensitivity Analysis	7
4. Conclusions	9
5. References	10
List of Symbols, Abbreviations, and Acronyms	13
Appendix. Deviation of Magnetic Alignment	15
Distribution List	17

List of Figures

Fig. 1	Schematic displaying the convergence of angles with respect to the magnetic field (θ) due to symmetry	3
Fig. 2	Effect of viscosity (η) on alignment time with varying applied magnetic field (B). For relevant system conditions of a 1.8-T applied magnetic field and a viscosity of 0.75–1.2 (N-s)/m ² , time necessary for alignment is predicted to be in the range of 35–55 s.....	5
Fig. 3	Effect of magnetic anisotropy ($\Delta\chi$) on alignment time with varying applied magnetic field (B). For relevant system conditions of a 1.8-T applied magnetic field and a $\Delta\chi$ of 8.92×10^{-12} , time necessary for alignment is predicted to be in the range of 50–60 s.	5
Fig. 4	Effect of particle radius (r) on alignment time with varying particle conductivity (σ). For relevant system conditions where particle conductivity is 0 or nearly 0, particle radius is predicted to have no effect.	6

List of Tables

Table 1	Sensitivity factors for process variables in the magnetic torque energy equation (Eq. 1). Higher values indicate higher model sensitivity, which highlights variables that are more effective for increasing material response to a magnetic field. $\Delta\chi$ denotes the magnetic susceptibility anisotropy, r denotes particle radius, and B denotes applied magnetic field strength.	8
Table 2	Sensitivity factors for process variables in the alignment time equation (Eq. 2). Higher values indicate higher model sensitivity, which highlight variables that are more effective for increasing the material response to a magnetic field. B denotes applied magnetic field strength, η denotes slurry viscosity, r denotes particle radius, and $\Delta\chi$ denotes the magnetic susceptibility anisotropy.....	8

1. Introduction

All materials, due to their atomic nature, have some magnetic response. However, for most materials, the response is so small that it is considered negligible. Magnetic susceptibility, χ , is a material property that indicates how strongly a material will magnetize in response to an applied magnetic field.¹ Consequently, it is also a measure of the field strength required for producing an appreciable response. For materials with exceptionally small magnetic susceptibilities, a significantly strong magnetic field is necessary to produce a response (2–10 T).^{2–6} This is the case for many ceramic materials (e.g., alumina), which are often paramagnetic or diamagnetic.^{2–6}

Many ceramics exhibit magnetic susceptibility anisotropy ($\Delta\chi$) with variations in magnetic susceptibility due to different crystallographic directions. Because of this anisotropy, crystals will align their axes with the highest magnetic susceptibility in the direction of the field that provides a mechanism for preferred orientation.^{3–9} The magnetic response of ceramics is governed by 2 main equations derived from first principles according to Sugiyama et al.¹⁰ Equation 1 describes the anisotropic magnetic energy (ΔE), or torque, acting on the particle due to its magnetic anisotropy as a function of the system properties and applied magnetic field.¹⁰ Equation 2 describes the temporal requirement (t) for rotation of the crystal, assuming no steric hindrance.¹⁰ It is derived by summing the effects of inertial, viscous, Lorentzian, and magnetization forces. Equation 2 assumes that the characteristic inertial response time is negligible compared with the viscous and Lorentzian times, which is valid for most small particles with moderate densities and viscosities.¹⁰ Full derivations are available in Sugiyama et al.,¹⁰ and an abbreviated derivation and adaptation of relevant equations is available in the Appendix for Eqs. 1 and 2.

$$\Delta E = V \frac{(\chi_c - \chi_{a,b})B^2}{2\mu_0} > k_B T \quad (1)$$

and

$$t = -\mu_0 \frac{30\eta + r^2 \sigma B^2}{5(\chi_c - \chi_{a,b})B^2} \ln \left(\frac{\tan \theta}{\tan \theta_0} \right), \quad (2)$$

where V is the primary crystal volume, $\chi_{a,b}$ and χ_c are the unitless magnetic susceptibilities of the crystallographic planes that are perpendicular and parallel to the magnetic field following alignment respectively, μ_0 is the permeability of free space, B is the externally imposed magnetic flux density, k_B is Boltzmann's constant, T is the absolute temperature, t is the time needed for a crystal to rotate a certain amount assuming no steric hindrances, η is the viscosity of the melt or fluid

surrounding the crystal, r is the crystallite radius, σ is the electrical conductivity of the particle, and Θ_0 and Θ are the initial and final angles of the crystal easy-axis (parallel axis, χ_c) with respect to the magnetic field, respectively.¹⁰ Historically, there is much confusion in the literature concerning these equations due to the use of several different sets of units for magnetic properties. The equations and derivations referenced in this report were confirmed for accuracy by performing dimensional analysis.

Using these equations, the magnetic torque applied to the particle and the time necessary for rotation can be estimated and used to predict the response of materials to strong magnetic fields. The sensitivity of such responses to small changes in input variables such as field strength and viscosity can also be assessed. This report presents predictions about the magnetic field response and sensitivity of process variables for alumina ceramics that are currently being investigated. However, the code and analysis developed for this application can easily be adapted to other material systems by changing the appropriate material properties.

2. Methods

2.1 Defining Parameters

For each process variable, representative values were gathered experimentally, from the literature, and from product data sheets. $\Delta\chi$ for pure alumina was calculated from the molar susceptibility, $\Delta\chi_m$, which was found to be 7.1×10^{-8} emu/mol.⁵ Since emu/mol is a nonstandard centimeter-gram-second electromagnetic unit (emu), it was first converted to SI (international standard) units of m^3/mol by multiplying by the conversion factor $4\pi \times 10^{-6}$.¹¹ Finally, molar susceptibility, $\Delta\chi_m$, was converted to unitless volume susceptibility, $\Delta\chi$, using Eq. 3.¹²

$$\Delta\chi_m = \Delta\chi_g FW = \frac{\Delta\chi}{\rho} FW \rightarrow \Delta\chi = \frac{\Delta\chi_m}{FW} \rho = V_m \Delta\chi_m, \quad (3)$$

where FW is formula weight, ρ is the theoretical density of the material, V_m is the molar volume of the material, and $\Delta\chi_g$ is the mass susceptibility.¹² Values for alumina were set at 0.10196 kg/mol [$2(26.98) + 3(16.00)$ g/mol] and 3990 kg/m³, respectively.¹³

Particle radius, r , was set at 150 nm to represent the nanosized powder currently being investigated. Particle volume, V , was calculated from the particle radius assuming spherical geometry. Temperature, T , was set at room temperature (298 K) and electrical conductivity, σ , was set to 0 (ohm-m)⁻¹ since the conductivity of alumina is negligible.¹⁴ Applied magnetic field strength, B , and medium

viscosity, η , were analyzed at 2 different values based on practical testing conditions. Field strength was analyzed at both 1.8 and 9 T (magnetic fields available for testing), and viscosity was analyzed at both 1.2¹⁵ and 0.75 Pa-s¹⁶ to mimic casting with epoxies and gel-casting slurries as the liquid mediums, respectively. Θ_0 and Θ were set to 89° and 1°, respectively. Considering that the range of possible angles before symmetry causes repetition (in terms of energy) is 0°–90° (see Fig. 1), it was determined that the maximum alignment time will occur when all particles are at 90° to the field direction. However, since the tangent function is undefined at 90°, the initial angle was set to 89° so that useful values could be calculated.¹⁰ For similar reasons, the final angle was set to 1° instead of 0°.¹⁰

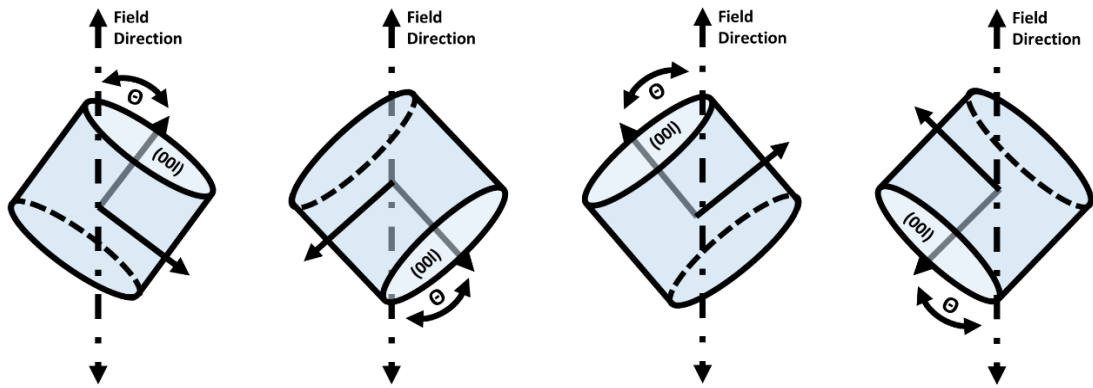


Fig. 1 Schematic displaying the convergence of angles with respect to the magnetic field (Θ) due to symmetry

2.2 Magnetic Response Predictions

The information and equations presented were coded into MATLAB functions for easy evaluation. Viscosity, field strength, particle radius, and magnetic susceptibility anisotropy (associated with changes in doping levels) were varied while holding all other variables constant within ranges relevant to the conditions presented for alumina with respect to alignment time.

2.3 Sensitivity Analysis

Using the same MATLAB functions from Section 2.2, sensitivity analysis was performed. Sensitivity analysis is commonly used when evaluating mathematical models of complex biological enzymatic pathways, but the principle is still useful for this application.^{17,18} Sensitivity, in modeling terms, is defined as the relative change in output compared with the relative change in input. Higher values of sensitivity are associated with larger impact for a specified variable. While this

indicates a lack of robustness in biological models, for mathematical models derived from first principles it identifies the most efficient parameters to target experimentally.¹⁸ In this analysis, each variable was systematically perturbed by decreasing it by 10% while holding all other variables constant. Since sensitivity analysis can only be conducted locally, relative to a baseline set of parameters, sensitivity was assessed at both 1.8 and 9 T and 0.75 and 1.2 (N-s)/m² to determine if the local sensitivity differed experimentally from purely theoretical inputs at values of interest. The times required for alignment or magnetic torque energy were recorded both before and after the perturbation, and the sensitivity function, *SOF*, was calculated according to Eq. 4.

$$SOF = \frac{(Output_{perturbed} - Output_{Baseline})}{(Output_{Baseline}) \times (perturbation\ amount)}, \quad (4)$$

where output indicates either ΔE (magnetic torque energy) or t (alignment time), and *perturbation amount* is the amount that the variable is reduced, which in this case is 0.1 (10%) for all analyses.¹⁷ A value of 10% perturbation was used to maintain locally relevant conditions within the model, as required when performing sensitivity analysis.¹⁸

3. Results and Discussion

3.1 Magnetic Response Predictions

The effects of viscosity on alignment time with varying applied magnetic field (Fig. 2) and the changes in magnetic anisotropy with varying magnetic field (Fig. 3) have been studied. As magnetic field increases, alignment occurs more rapidly. Increasing viscosity also increases the time necessary for alignment but is not as effective as the influence of a magnetic field. Increasing magnetic anisotropy also decreases the alignment time significantly, as expected. However, since it is unknown how much the magnetic anisotropy of alumina is affected by different dopants and dopant concentrations, it is also unknown how relevant this will factor will be experimentally.

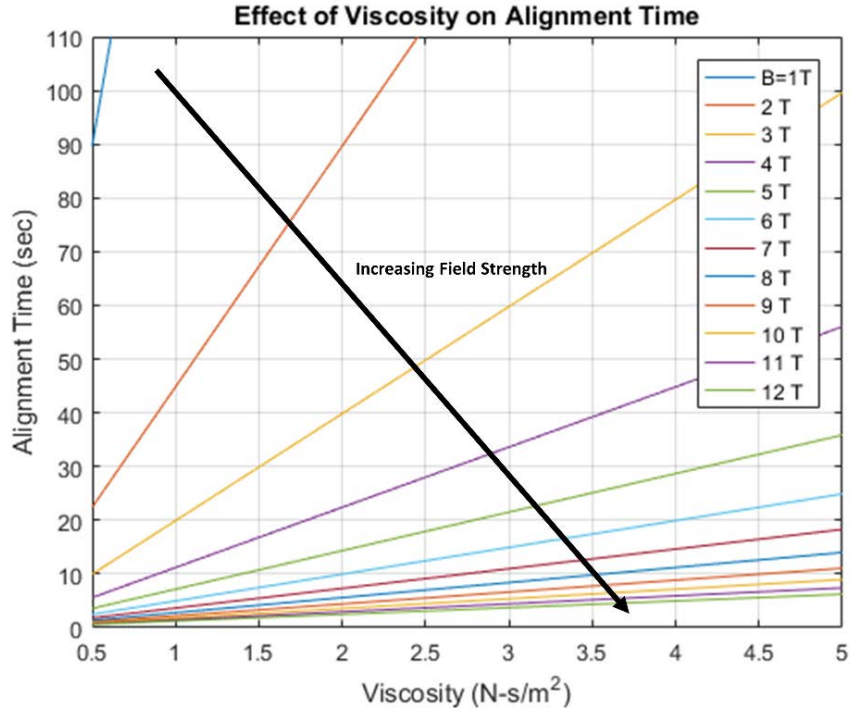


Fig. 2 Effect of viscosity (η) on alignment time with varying applied magnetic field (B). For relevant system conditions of a 1.8-T applied magnetic field and a viscosity of 0.75–1.2 (N-s)/m², time necessary for alignment is predicted to be in the range of 35–55 s.

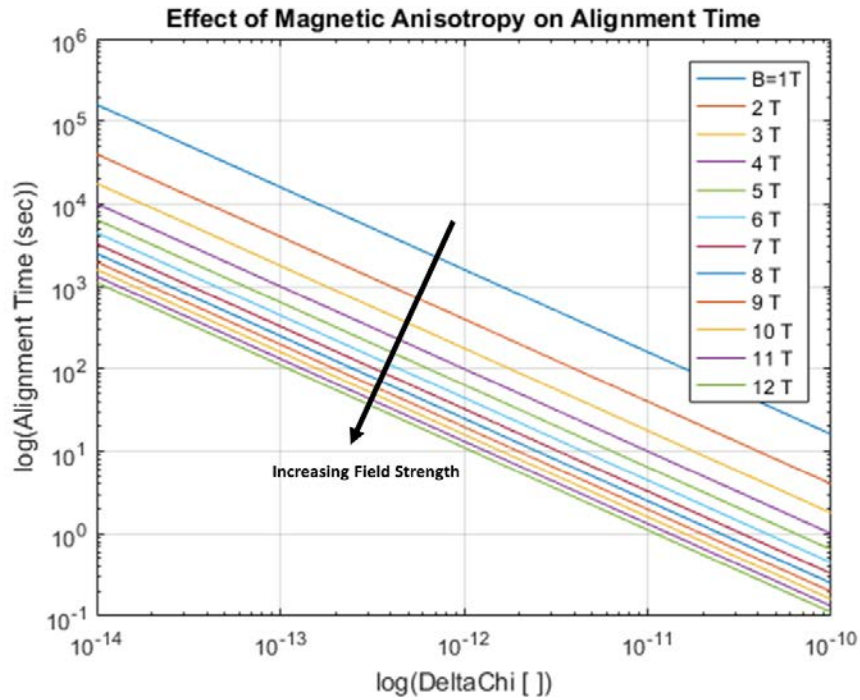


Fig. 3 Effect of magnetic anisotropy ($\Delta\chi$) on alignment time with varying applied magnetic field (B). For relevant system conditions of a 1.8-T applied magnetic field and a $\Delta\chi$ of 8.92×10^{-12} , time necessary for alignment is predicted to be in the range of 50–60 s.

Figure 4 shows the effect of particle radius on alignment time with varying electrical conductivity. As conductivity increases, alignment time increases with an increase in the Lorentzian force component that opposes rotation. The Lorentz force arises when current induced by the magnetic field interacts with the field itself, inducing electromagnetic force on the particles. This force works in the opposite direction of the magnetic torque forces and can be thought of as a “magnetic inertia” that must be overcome for alignment to occur. The induced current increases with increasing electrical conductivity such that higher-conductivity materials experience higher Lorentz forces. However, it should be noted that when the conductivity is zero, as in the case of alumina, particle radius has no effect on alignment time.

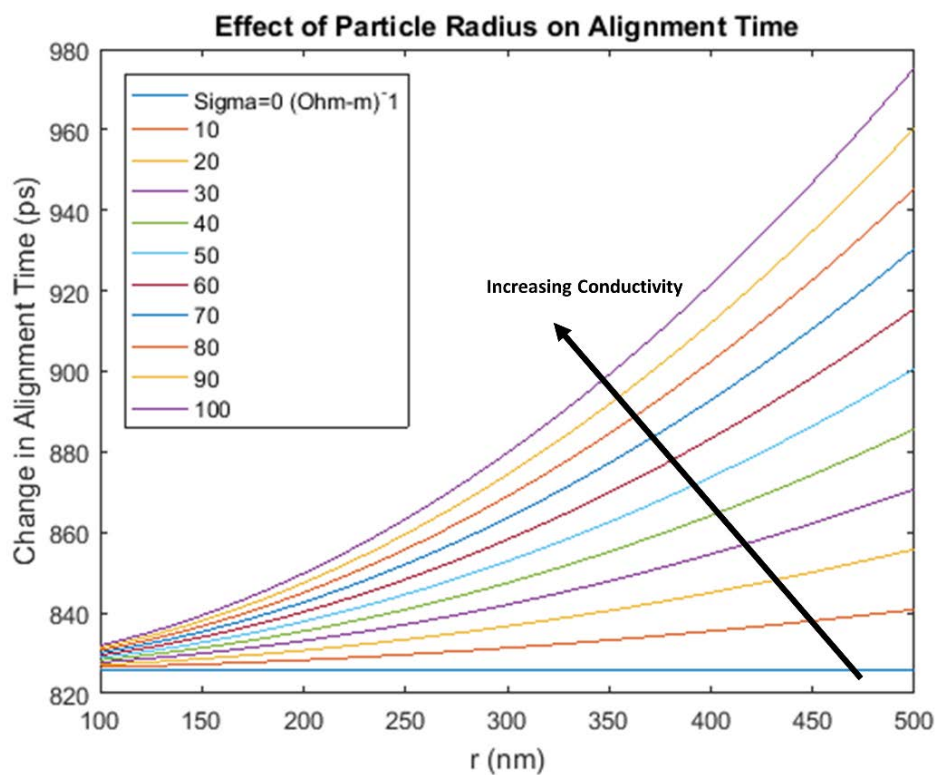


Fig. 4 Effect of particle radius (r) on alignment time with varying particle conductivity (σ). For relevant system conditions where particle conductivity is 0 or nearly 0, particle radius is predicted to have no effect.

While it is unknown how much dopant identity and concentration will affect overall conductivity, the values presented in Fig. 4 are well outside the range of any reasonable change, particularly for most ceramic materials of any composition.¹⁹ The reason such a large variety of conductivity values was used was to produce changes in alignment time significant enough to show the effect of particle radius and conductivity. Looking at the scale on the y-axis in Fig. 4, alignment time only varies by 12×10^{-11} s with a 100-fold change in conductivity. This indicates that in

the case of almost all ceramic materials, the Lorentzian force component of the magnetic alignment equations (and associated variables) can be considered negligible as has been proposed previously.²⁰ This is particularly evident in the context of parameters such as magnetic field strength and anisotropy, which have a much stronger influence over alignment time. Additionally, simulations were performed for both silver and graphene, which are known as some of the most conductive materials available ($\sigma = 3.5 \times 10^7$ [ohm-m]⁻¹ and 2.05×10^7 [ohm-m]⁻¹, respectively²¹), and changes in alignment time due to particle radius were still only on the order of 2 s. For this reason, it was concluded that for powder samples of almost any material, variations due to changes in conductivity and particle radius can be neglected, especially when the set times are on the order of tens of minutes.

For the levels of applied magnetic field, viscosity, magnetic anisotropy, conductivity, and particle radius relevant to alignment of alumina in a 1.8-T magnetic field with low-viscosity slurries, the simulations predict necessary alignment times of approximately 30–50 s, which is well within the range of experimental conditions. However, the simulations do not take into account possible steric interactions between particles that have been shown to prevent complete alignment for irregularly shaped particles.²² This is an issue particularly when using particles of plate or needle-like morphologies that can pin each other during the rotation process, creating particle bridges that prevent further rotation. This inhibitory effect will only increase with the solids loading of the slurries, as there will be even less room for particles to freely rotate.

In addition, the simulations do not address the possibility that agglomerates have many crystals with opposing domains that may conflict with each other during alignment. Since the current powders are not milled or de-agglomerated in any significant way before processing, it is very likely that they are highly agglomerated, resulting in less-effective alignment. These simulations also do not take into account changes in magnetic torque based on variations in particle shape, which is known to affect magnetic response.^{23–25} Given that the predicted times are on the order of tens of seconds, it is still anticipated that some degree of alignment will be achievable, as the setting times for epoxy and gel-casting slurries range from 30 min to several hours. This is also supported by preliminary results.²⁶

3.2 Sensitivity Analysis

The calculated sensitivity functions (SOFs) for parameters in the magnetic torque energy and alignment time equations (Eqs. 1 and 2) are shown in Tables 1 and 2 for the 1.8- and 9-T magnetic fields and the 0.75- and 1.2-(N-s)/m² baseline viscosities, respectively. In both models, the local sensitivity is exactly the same

for all cases of experimental interest. This was expected because the model was derived from first principles instead of empirically, which can introduce unexpected and unrealistic outputs in extrapolated regions. Instantaneous sensitivity (not normalized to the baseline) was calculated analytically at values of 1.8 T and 0.75 (N-s)/m² using partial derivatives. The resulting SOF values (data not shown) showed similar trends but much higher magnitudes compared with the data in Table 2, which supports the validity of this method. However, since the local normalized sensitivity values relative to variations that could occur naturally in a practical setting are much more valuable than instantaneous theoretical sensitivities, the method previously presented is considered to be more relevant.

Table 1 Sensitivity factors for process variables in the magnetic torque energy equation (Eq. 1). Higher values indicate higher model sensitivity, which highlights variables that are more effective for increasing material response to a magnetic field. $\Delta\chi$ denotes the magnetic susceptibility anisotropy, r denotes particle radius, and B denotes applied magnetic field strength.

Variable	Sensitivity Function (SOF)	
	1.8 T	9 T
$\Delta\chi$	1	1
r	2.71	2.71
B	1.9	1.9

Table 2 Sensitivity factors for process variables in the alignment time equation (Eq. 2). Higher values indicate higher model sensitivity, which highlight variables that are more effective for increasing the material response to a magnetic field. B denotes applied magnetic field strength, η denotes slurry viscosity, r denotes particle radius, and $\Delta\chi$ denotes the magnetic susceptibility anisotropy.

Variable	Sensitivity Function (SOF)			
	1.8 T		9 T	
	0.75 (N-s)/m ²	1.2 (N-s)/m ²	0.75 (N-s)/m ²	1.2 (N-s)/m ²
B	2.35	2.35	2.35	2.35
η	1.00	1.00	1.00	1.00
r	0.00	0.00	0.00	0.00
$\Delta\chi$	1.11	1.11	1.11	1.11

As shown in Table 2, when considering the parameters that affect alignment time, the strength of the applied magnetic field (B) has the most influence. Magnetic anisotropy ($\Delta\chi$) and viscosity (η) also affect the alignment time but not as drastically as field strength. This was also reflected in Figs. 1 and 2, as described. The particle radius has a sensitivity factor of zero and therefore has no effect on alignment time when particles are nonconductive as discussed previously.

While of little experimental relevance, the sensitivity of magnetic torque energy to various process variables is displayed in Table 1. In contrast with alignment time,

particle radius has the highest impact on magnetic torque, followed by field strength and magnetic anisotropy. While seemingly counterintuitive, the mathematical reason for this phenomena is easily explained. When volume is expressed as a function of r^3 and combined with the viscous and Lorentz force terms, it is simply canceled out, as shown in the Appendix (Eqs. 10 and 11). Conceptually, the reason is not as obvious. Volume does not translate directly to shorter alignment times because its advantage is offset by a viscous force term in which the resistance to torque is proportional to the increase in volume. Therefore, this term does not appear in the final alignment time equation (Eq. 2).

4. Conclusions

Simulations predict that alignment will be possible under the imposed experimental conditions. Furthermore, when dopants are added to enhance the magnetic anisotropy ($\Delta\chi$), the alignment response will increase. Previous literature cites field strengths in excess of 10 T necessary for alignment,^{5,6} but according to these simulations, it appears that lower strength fields are sufficient for alignment. Preliminary experimental evidence²⁶ and some literature²⁷ appear to support this,²³ but more work is required to confirm that lower fields are indeed sufficient to observe statistically significant alignment for alumina-based ceramics. It is possible that the equations derived from first principles simply do not take into account other practical considerations, such as the aforementioned interparticle interactions,²² and conclusions regarding alignment time are not applicable.

The sensitivity analysis indicates that the strongest parameter affecting magnetic alignment is the strength of the applied magnetic field (B). This means that in experimental applications the most effective way to increase alignment is to increase the magnetic field. However, this also means that every precaution must be taken to ensure that field is stable and consistent before commencing experiments. At the very least, the instability of the field must be monitored to quantify uncertainty, as this is likely the most prevalent source of variability. Viscosity and magnetic susceptibility anisotropy ($\Delta\chi$) were also shown to have an impact on overall alignment, but their effects were less pronounced than changes in field strength. While it was not a source of variability within experiments, analysis of the sensitivity indicated that changes in anisotropy affect alignment response, thus variations in alignment at lower field strengths with different dopants are also expected.

5. References

1. Schenck JF. The role of magnetic susceptibility in magnetic resonance imaging: MRI magnetic compatibility of the first and second kinds. *Medical Physics*. 1996;23(6):815–850.
2. Libanori R, Reusch FB, Erb RM, Studart AR. Ultrahigh magnetically responsive microplatelets with tunable fluorescence emission. *Langmuir*. 2013;29(47):14674–14680.
3. Sun ZHI, Guo X, Guo M, Vleugels J, Van der Biest O, Blanpain B. Alignment of weakly magnetic metals during solidification in a strong magnetic field. *Journal of Alloys and Compounds*. 2013;551:568–577.
4. Terada N, Suzuki HS, Suzuki TS, Kitazawa H, Sakka Y, Kaneko K, Metoki N. In situ neutron diffraction study of aligning of crystal orientation in diamagnetic ceramics under magnetic fields. *Applied Physics Letters*. 2008;92(3):112507.
5. Terada N, Suzuki HS, Suzuki TS, Kitazawa H, Sakka Y, Kaneko K, Metoki N. Neutron diffraction texture analysis for α - Al_2O_3 oriented by a high magnetic field and sintering. *Journal of Physics D – Applied Physics*. 2009;42(10).
6. Zhang L, Vleugels J, Van der Biest O. Slip casting of alumina suspensions in a strong magnetic field. *Journal of the American Ceramic Society*. 2010;93(10):3148–3152.
7. Suzuki TS, Sakka Y, Kitazawa K. Orientation amplification of alumina by colloidal filtration in a strong magnetic field and sintering. *Advanced Engineering Materials*. 2001;3(7):490–492.
8. Makiya A, Shouji D, Tanaka S, Uchida N, Kimura T, Uematsu K. Grain oriented microstructure made in high magnetic field. *Key Engineering Materials*. 2002;206–213:445–448.
9. Gillon P. Uses of intense DC magnetic field in material processing. *Materials Science and Engineering A*. 2000;287(2):146–152.
10. Sugiyama T, Tahashi M, Sassa K, Asai S. The control of crystal orientation in non-magnetic metals by imposition of a high magnetic field. *Iron and Steel Institute of Japan International*. 2003;43(6):855–861.
11. Goldfarb RB, Fickett FR. Units for magnetic properties. Boulder (CO): National Bureau of Standards (US); 1985 Mar. NBS Special Publication 696.

12. Figgis BN, Lewis J. In: Lewis J, Wilkins RG, editors. Modern coordination chemistry. New York (NY): Interscience Publishers Inc.; 1960. p. 400–454.
13. Park J. Bioceramics: properties, characterizations and applications. New York (NY): Springer Science and Business Media; 2009. Chapter 6. p. 120.
14. Auerkari P. Mechanical and physical properties of engineering alumina ceramics. Espoo (Finland): VTT Technical Research Centre of Finland; 1996. Research Notes 1792.
15. Technical Data Sheet EP1112NC Clear. Germantown (WI): Resinlab [accessed 2016 July 20]. <http://resinlab.com/images/resources/pdf/TDS08043.pdf>.
16. Takai C, Tsukamoto M, Fuji M, Takahashi M. Control of high solid content yttria slurry with low viscosity for gelcasting. *Journal of Alloys and Compounds*. 2006;408–412:533–537.
17. Aldridge BB, Burke JM, Laffenburger DA, Sorger PK. Physicochemical modelling of cell signaling pathways. *Nature Cell Biology*, 2006;8(11):1195–1203.
18. Bentele M, Lavrik I, Ulrich M, Stober S, Heermann DW, Kalthoff H, Krammer PH, Eils R. Mathematical modeling reveals threshold mechanism in CD95-induced apoptosis. *Journal of Cell Biology*. 2004;166(6):839–851.
19. Granta Design, Ltd. CES software 2009 edupack: 2 material and process selection charts. Version MFA 09. Cambridge (UK): Granta Design Ltd; 2009.
20. Sun ZHI, Guo M, Vleugels J, Van der Biest O, Blanpain B. Processing of non-ferromagnetic materials in strong static magnetic field. *Current Opinion in Solid State and Materials Science*. 2013;17(4):193–201.
21. Materials Science and Engineering Dept., Drexel University. CES selector 2010. Cambridge (UK): Granta Design Ltd; 2010.
22. Makiya A, Shouji D, Tanaka S, Uchida N, Kumura T, Uematsu K. Grain oriented microstructure made in high magnetic field. *Key Engineering Materials*. 2002;206–213:445–448.
23. Song Q, Zhang ZJ. Shape control and associated magnetic properties of spinel cobalt ferrite nanocrystals. *Journal of the American Chemical Society*. 2004;126(19):6164–6168.
24. Batlle X, Labarta A. Finite-size effects in fine particles: magnetic and transport properties. *Journal of Physics D: Applied Physics*. 2002;35(6):R15–R42.

25. Issa B, Obaidat IM, Abiss BA, Haik Y. Magnetic nanoparticles: surface effects and properties related to biomedicine applications. *International Journal of Molecular Science*. 2013;14(11):21266–21305.
26. Moorehead C, Blair V, Limmer K, Brennan R, Adams J. Preferred orientation of rare-earth doped alumina crystallites by and applied magnetic field. Aberdeen Proving Ground (MD): Army Research Laboratory (US); 2016 June. Report No.: ARL-TR-7702.
27. Uyeda C, Takashima R, Tanaka K. Magneto-rotation of non-magnetic micro-crystals caused by diamagnetic anisotropy. *Applied Physics Letters*. 2005;86:094103.

List of Symbols, Abbreviations, and Acronyms

$\chi_{a,b}, (\kappa_{a,b})$	volume magnetic susceptibility of crystallographic planes perpendicular to the applied magnetic field
$\chi_c (\kappa_c)$	volume magnetic susceptibility of crystallographic plane parallel with the applied magnetic field
$\Delta\chi (\Delta\kappa)$	volume magnetic susceptibility anisotropy associated with a material, calculated as $\chi_c - \chi_{a,b}$,
B	applied magnetic field [T]
T	temperature [K]
η	solution viscosity [(N-s)/m ²]
t	time needed for crystal rotation [s]
k_B	Boltzmann's constant, 1.381×10^{-23} [J/k]
μ_0	permeability of vacuum, $4\pi \times 10^{-7}$ [(T-m)/A]
r	crystal radius (assumes spherical particles) [m]
σ	electrical conductivity of the particles [(Ω -m) ⁻¹]
V	primary crystal volume [m ³]
Θ	final angle of magnetic easy-axis (c-axis) with respect to magnetic field axis [°]
Θ_0	initial angle of magnetic easy-axis (c-axis) with respect to magnetic field axis [°]
ΔE	energy/torque associated with magnetic anisotropy [J] or [N-m]
ΔX_m	molar magnetic susceptibility anisotropy associated with a material [m ³ /mol]
ΔX_g	mass magnetic susceptibility anisotropy associated with a material [m ³ /kg]
V_m	molar density [mol/m ³]
ρ	theoretical density associated with a material [kg/m ³]
FW	formula weight associated with a material [kg/mol]
SOF	sensitivity function: how much that parameter affects the outcome of a model

INTENTIONALLY LEFT BLANK.

Appendix. Deviation of Magnetic Alignment

As adapted from Sugiyama et al.,¹ 4 kinds of forces are active when aligning particles in a magnetic field: 1) inertial force, 2) viscous force, 3) Lorenz force, and 4) magnetization force. Equations for each of these active forces are presented in Eqs. A-1 through A-8.

$$\text{Inertia Force:} \quad \frac{2}{5} \rho r^5 \frac{d^2 \theta}{dt^2}. \quad (\text{A-1})$$

$$\text{Viscous Force:} \quad 8\pi\eta r^3 \frac{d\theta}{dt}. \quad (\text{A-2})$$

$$\text{Lorenz Force:} \quad \frac{4}{15} \pi r^5 \frac{d\theta}{dt}. \quad (\text{A-3})$$

$$\text{Magnetization Force:} \quad \frac{1}{2\mu_0} V \Delta\chi B^2 \sin(2\theta). \quad (\text{A-4})$$

Summing all torque forces acting on particles under a magnetic field results in Eq. A-5, which is consequently solved to produce the equation for alignment time as presented in Eq. 2 in the main report. Eq. A-5 is simply the sum of main report Eqs. 5–8.

$$\frac{2}{5} \rho r^5 \frac{d^2 \theta}{dt^2} + 8\pi\eta r^3 \frac{d\theta}{dt} + \frac{4}{15} \pi r^5 \frac{d\theta}{dt} + \frac{1}{2\mu_0} r^3 \Delta\chi B^2 \sin(2\theta) = 0. \quad (\text{A-5})$$

As stated, since the particles are small and the viscosity and particle material density in question (alumina) moderate, the inertia force term can be neglected since under those circumstances the characteristic response time will be much smaller than the contribution of the other forces. Neglecting the inertial term yields Eq. A-6:

$$8\pi\eta r^3 \frac{d\theta}{dt} + \frac{4}{15} \pi r^5 \frac{d\theta}{dt} + \frac{1}{2\mu_0} r^3 \Delta\chi B^2 \sin(2\theta) = 0, \quad (\text{A-6})$$

which upon simplification results in Eq. A-7, which is the instance where particle volume, expressed as r^3 in the magnetization term, is mathematically removed from the alignment time equation.

$$8\pi\eta \frac{d\theta}{dt} + \frac{4}{15} \pi r^2 \frac{d\theta}{dt} + \frac{1}{2\mu_0} \Delta\chi B^2 \sin(2\theta) = 0. \quad (\text{A-7})$$

Solving the differential equation yields Eq. A-8, which when the appropriate substitutions are made, exactly corresponds to Eq. 19 in Sugiyama et al.,¹ where the authors have chosen to lump all material parameters into a term, τ .

$$\tan(\theta) = \tan(\theta_0) \exp\left(-\frac{5t\Delta\chi B^2}{(30\eta + r^2\sigma B^2)\mu_0}\right). \quad (\text{A-8})$$

Eq. A-8, upon rearranging to solve for t , yields Eq. 2 in the main report.

¹Sugiyama T, Tahashi M, Sassa K, Asai S. The control of crystal orientation in non-magnetic metals by imposition of a high magnetic field. Iron and Steel Institute of Japan International. 2003;43(6):855–861.

1 DEFENSE TECHNICAL
(PDF) INFORMATION CTR
DTIC OCA

2 DIRECTOR
(PDF) US ARMY RESEARCH LAB
RDRL CIO L
IMAL HRA MAIL & RECORDS
MGMT

1 GOVT PRINTG OFC
(PDF) A MALHOTRA

4 DIR USARL
(PDF) RDRL WMM D
M KORNECKI
RDRL WMM E
V BLAIR
C MOOREHEAD
R BRENNAN

INTENTIONALLY LEFT BLANK.